# Propagation of plane waves and of waveguide modes in quasiperiodic dielectric heterostructures

R. Pelster,* V. Gasparian,† and G. Nimtz
*II. Physikalisches Institut der Universität zu Köln, Zülpicher Straße 77, 50676 Köln, Germany*
(Received 19 December 1996)

We study the propagation of electromagnetic waves in one-dimensional quasiperiodic systems and its dispersion relation for plane waves and for waveguide structures. In the photonic band gaps, periodic, Fibonacci, and Thue-Morse multilayer systems can be described by a complex effective wave vector. Its negative imaginary part causes an exponential decay of the transmission coefficient due to a distributed quasitotal reflection. Its real part is independent of frequency, so that the phase time becomes independent of the system size. This time alternates between two distinct values and approximately equals the Büttiker-Landauer tunneling time. Superluminal group velocities are obtained for the propagation of narrow frequency band wave packets. The effective complex wave vector results from multiple reflections of oscillating propagating waves. For both the plane wave and the waveguide dispersion the most ordered structures exhibit the most effective coherent interference and thus the deepest gaps in the transmission spectra as well as the smallest decay length. The Thue-Morse sequence is less ordered than the Fibonacci one, which in turn is less ordered than the periodic system. Increasing disorder enhances the phase time, the Büttiker-Landauer time, and the density of states in the gap regions. The group velocity becomes smaller, but still remains superluminal. The spectra of $\lambda/4$ systems are similar for both the plane-wave and the waveguide dispersion. The Fibonacci scaling relation has been checked. It holds for a periodicity of 6, whereas the claimed periodicity of 3 has found to be not valid in general. [S1063-651X(97)00506-0]

PACS number(s): 42.70.Qs, 41.20.Jb, 42.25.Hz, 71.55.Jv

## I. INTRODUCTION

A lot of work has been carried out to study energy spectra of quasiparticles [1–5], thermodynamic properties [6,7], and electronic and electromagnetic wave propagation [8,9] in one-dimensional quasiperiodic systems, e.g., in chains of two building blocks alternating according to a Fibonacci or a Thue-Morse sequence. In this intermediate regime between order and disorder also ''band gaps'' occur in the transmission spectra analogous to periodic electronic structures. The absence of propagating modes is caused by coherent multiple scattering and interference of partial waves, i.e., it occurs on a scale of the wavelength. While infinite periodic systems exhibit complete photonic band gaps, positional disorder creates pseudogaps of localized states [10]. These are modified in the intermediate quasiperiodic regime. For example, the scaling properties of self-similar quasiperiodic Fibonacci spectra have been interpreted as a sign for quasilocalization [8,9], i.e., the decay of the wave functions is less than exponential. Until now, as far as we know, mainly plane waves have been considered. This case corresponds, for example, to a light beam propagating through a dielectric multilayer system. Another experimental realization might be a TE mode in a material-filled coaxial cable.

In telecommunication engineering waveguide structures are important, e.g., for the transmission of microwave signals or for optical signals between integrated microchips on wafers. Due to the boundary conditions, the propagation of the guided wave is altered compared with a plane wave. The dispersion relation of the wave vector changes and thus also the frequency spectra of the complex transmission and reflection coefficients. In this work we study the consequences for Thue-Morse, Fibonacci, and periodic systems. From the complex transmission coefficient quantities such as decay length, phase time, Büttiker-Landauer tunneling time, density of states, and group velocity are calculated, all of which reflect the degree of order of the respective system. In the gap regions the interaction time of a wave with the potential barrier is of special interest. We discuss the question of how much time tunneling takes and the superluminal barrier traverse involved.

## II. CALCULATION OF THE TRANSMISSION SPECTRA

In a rectangular $H_{10}$ waveguide filled with a material (complex permittivity $\varepsilon$ and permeability $\mu$) propagates a TE mode with wave number

$$k=\frac{\omega}{c}\sqrt{\varepsilon\mu-(\nu_c/\nu)^2} \tag{1}$$

(for complex $k$ the convention $\mathrm{Im}[k]\leqslant 0$ determines the sign of the square root). The dispersion relation differs from that of a plane wave (TEM mode) by a nonvanishing cutoff frequency $\nu_c$. For an $X$-band waveguide (width $w=22.86$ mm, height $h=10.16$ mm) $\nu_c=c/2w=6.56$ GHz.

Consider a dielectric layer of thickness $d$ and wave impedance [11] $Z_m=Z_0\mu k_0/k$ ($Z_0$ and $k_0$ denote the wave impedance and wave number of the vacuum, respectively). In the case of normal incidence the complex reflection coefficient of a single interface is [11]

*Electronic address: rolf@obelix.ph2.uni-koeln.de
†Present address: Departamento de Electronica y Tecnologia de Computadores, Facultad de Ciencias, Universidad de Granada, 18071 Granada, Spain. Permanent address: Department of Physics, Yerevan State University, 375049, Yerevan, Armenia.

 

$$r=\frac{Z_m-Z_0}{Z_m+Z_0}=\frac{\mu k_0/k-1}{\mu k_0/k+1}. \tag{2}$$

Taking into account multiple reflections inside the layer, its transmission coefficients for the respective direction of propagation ($2\leftarrow 1$ or $1\leftarrow 2$) are [11,12]

$$S_{21}=S_{12}=\frac{(1-r^2)a}{1-a^2r^2} \tag{3}$$

and the corresponding reflection coefficients

$$S_{11}=S_{22}=\frac{(1-a^2)r}{1-a^2r^2}, \tag{4}$$

where $a$ is defined as

$$a=\exp(-ikd). \tag{5}$$

Thus the same functional relationship $S_{ij}(k,k_0)$ holds for the $S$ parameters for both the plane wave and the waveguide case.

In order to obtain the $S$ parameters of a multilayer system, the transmission matrices of the individual layers have to be calculated [13]:

$$\mathbf{T}_i=\begin{pmatrix} -S_{11}S_{22}/S_{21}+S_{12} & S_{11}/S_{21} \\ -S_{22}/S_{21} & 1/S_{21} \end{pmatrix}. \tag{6}$$

The transmission matrix of the whole system is obtained by multiplying the individual layer matrices

$$\mathbf{T}_{\rm sys}=\prod_i \mathbf{T}_i$$

according to a chosen sequence. In the following $t$ and $\varphi$ denote the amplitude and phase of the transmission coefficient of the system:

$$S_{21}^{\rm sys}=1/T_{22}^{\rm sys}=t\exp(-i\varphi). \tag{7}$$

We are going to compare three sequences consisting of two building blocks with transmission matrices $\mathbf{T}_a$ and $\mathbf{T}_b$: The periodic sequence

$$\mathbf{T}_{2i}=\mathbf{T}_{2i-1}\cdot\mathbf{T}_a, \quad \mathbf{T}_{2i+1}=\mathbf{T}_{2i}\cdot\mathbf{T}_b \quad (\mathbf{T}_0=\mathbf{T}_a),$$

the quasiperiodic Fibonacci sequence

$$\mathbf{T}_{i+1}=\mathbf{T}_i\cdot\mathbf{T}_{i-1} \quad (\mathbf{T}_0=\mathbf{T}_b,\ \mathbf{T}_1=\mathbf{T}_a), \tag{8}$$

and the quasiperiodic Thue-Morse sequence

$$\mathbf{T}_{i+1}=\mathbf{T}_i\cdot\mathbf{T}_i^* \quad (\mathbf{T}_0=\mathbf{T}_a\cdot\mathbf{T}_b)$$

(with $\mathbf{T}_i^*$ being the complement of $\mathbf{T}_i$, i.e., having interchanged building blocks $A$ and $B$). As a test we compare calculated and measured waveguide spectra of the Fibonacci element $F_5$, i.e., $ABAABABA$, in Fig. 1. Material $A$ was a Plexiglas layer ($d_a=5.9$ mm, $\varepsilon_a=2.6$), whereas layer $B$ was air ($d_b=9.5$ mm, $\varepsilon=1$). We have measured the transmission

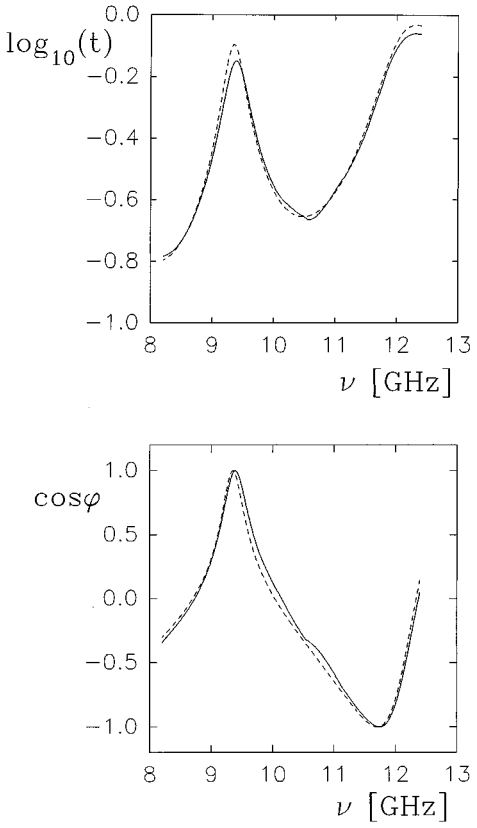


FIG. 1. Amplitude and phase of the transmission coefficient vs frequency for the Fibonacci element $F_5$ in an $X$-band waveguide (layer A: Plexiglas, $d_a=5.9$ mm, $\varepsilon_a=2.6$; layer B: air, $d_b=9.5$ mm). Solid lines, experiment; dashed lines, calculation.

coefficient of the waveguide using a Hewlett Packard 8510 B network analyzer and a Through-Reflect-Line calibration [14].

For coherent multiple scattering and thus for strong quasiperiodicity the effective lengths of both layers should be a multiple of a quarter wavelength [9], i.e.,

$$d_a\sqrt{\varepsilon_a\mu_a-(\nu_c/\nu)^2}=d_b\sqrt{\varepsilon_b\mu_b-(\nu_c/\nu)^2}=\frac{\lambda}{4}(2n+1) \tag{9}$$

($\nu_c=0$ for plane waves), i.e., both layers have the same phase length $kd$. Thus the center frequency of a transmission spectrum is

$$\nu_{\rm center}=\frac{1}{\sqrt{\varepsilon_a\mu_a}}\sqrt{\left(\frac{(2n+1)c}{4d_a}\right)^2+\nu_c^2} \tag{10}$$

and its corresponding frequency period is $[\nu_{\rm center}2n/(2n+1)\ ,\nu_{\rm center}(2n+2)/(2n+1)]$. In order to compare the plane-wave and the waveguide spectra, the material parameters $\varepsilon$ and $\mu$, the layer thickness, and the frequency range have to be chosen with respect to the following points: (a) The calculation of transmission matrices is only possible above the cutoff frequency of the feeding waveguide, i.e., in our case the empty $X$-band waveguide with $\nu_c=6.56$ GHz, and (b) the frequency period of the spectra should not be too large since the transmission spectra for

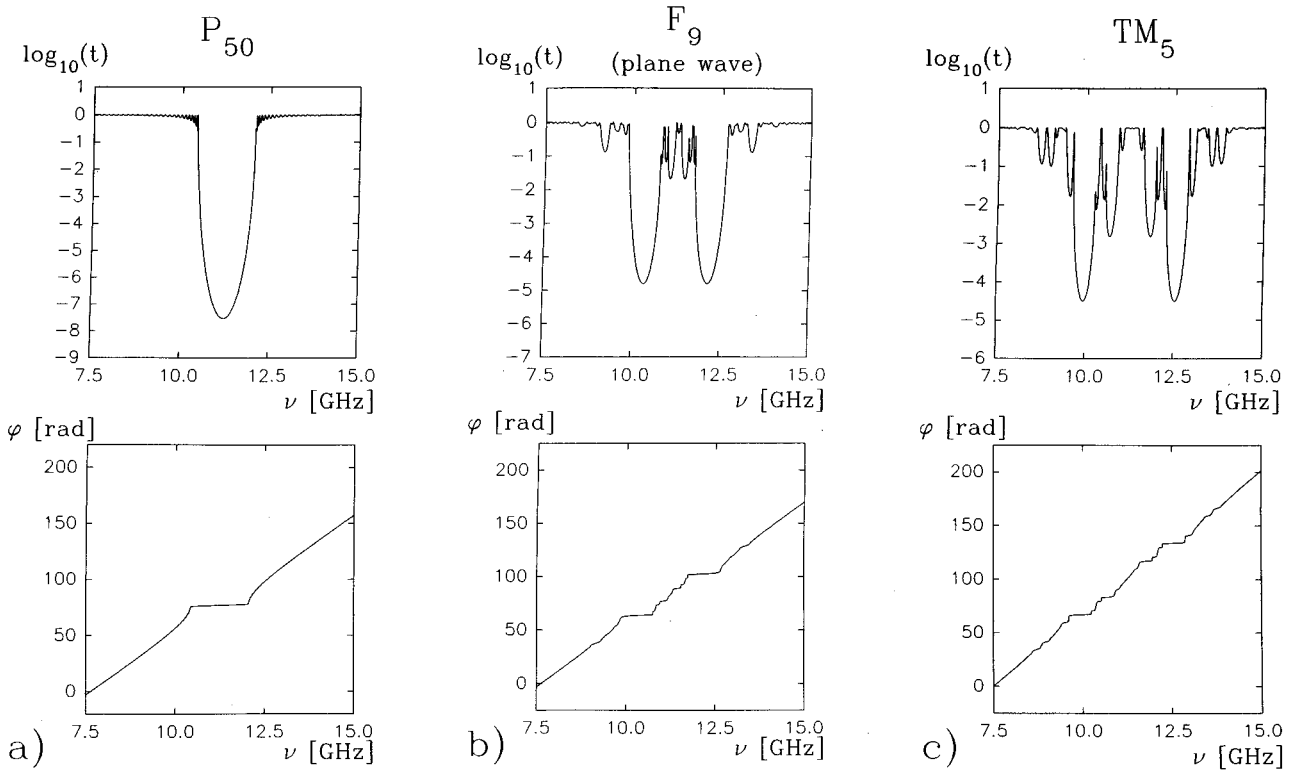


FIG. 2. Transmission coefficient vs frequency for the plane-wave dispersion: (a) periodic element $P_{50}$ ($L=0.76$ m), (b) Fibonacci element $F_9$ ($L=0.76$ m), and (c) Thue-Morse element $TM_5$ ($L=0.96$ m). At the center frequency Eq. (9) holds.

plane waves and waveguide modes differ mainly near $\nu_c$ and become similar at higher frequencies [see Eq. (1)].

## III. RESULTS

### A. Spectra and decay lengths

For the following calculations layer $T_a$ is supposed to be a nonmagnetic ($\mu_a=1$) loss-free dielectric material and layer $T_b$ corresponds to air ($\varepsilon_b=\mu_b=1$). First we choose

$$d_a=10 \text{ mm}, \quad \varepsilon_a=4-i0, \quad d_b=20 \text{ mm}.$$

These are 3/4-wavelength layers for a plane wave ($\nu_c=0$) with a center frequency of 11.242 GHz [Eq. (10) with $n=1$] and a period of 7.495–14.989 GHz. Of course, arranging the same layers in a waveguide does not yield a quarter-wavelength system [see Eq. (9) with $\nu_c=6.56$ GHz] and we can expect deviations in the spectra. (We assume that also above 12.4 GHz only the dominant $H_{10}$ mode propagates in the waveguide. This implies a perfect geometry of the multilayer system to avoid the excitation of higher modes.)

Figure 2 shows the transmission coefficient of the plane-wave dispersion for elements of different sequences having comparable lengths: the periodic element $T_{50}^{p}$ (51 elements, $L=0.76$ m), the Fibonacci element $T_9^F$ (55 layers, $L=0.76$ m) and the Thue-Morse element $T_5^{\mathrm{TM}}$ (64 layers, $L=0.96$ m). Figure 3 displays the spectra of the same systems ($d_a=10$ mm, $\varepsilon_a=4$, and $d_b=20$ mm) for the waveguide dispersion. Due to the altered dispersion relation and since the quarter-wavelength condition (9) does not hold, the waveguide spectra lose their symmetry. The gaps become deeper and additional ones appear. This can be understood easily. Let us consider the most simple spectrum, the periodic one. In the case of lossless material and plane waves the reflection coefficient of a single interface $r$ is independent of frequency [see Eq. (2)] and minima in the transmission coefficient of a single layer [Eq. (3)] only appear for $\exp(-2kd)=1$, i.e., the quarter-wavelength condition (9) with $n=1$. Thus the gap appears at the center frequency [Eq. (10) and Fig. 2(a)]. For the waveguide dispersion relation the peak position changes since Eq. (9) yields 11.7 GHz for layer $A$ and 13 GHz for layer $B$. In fact, the main gap appears near the mean value 12.35 GHz [see Fig. 3(a)]. These minima are caused by multiple reflections inside single layers. Increasing the system length enhances the effective reflection and the gaps become deeper (see below). A second mimimum appears near 9 GHz in the waveguide spectrum. It does not show up in a single-layer spectrum or in a real 3/4-wavelength waveguide spectrum and corresponds to a half wavelength. It is caused by multiple reflections between different layers and it is also observed at a similar position in the Fibonacci and Thue-Morse spectra.

For a given system length the depth of the gaps differs between Thue-Morse, Fibonacci, and periodic sequence (see Figs. 2 and 3):

$$t_{\min}^{\text{Thue-Morse}} > t_{\min}^{\text{Fibonacci}} > t_{\min}^{\text{periodic}}. \tag{11}$$

This holds for the plane-wave dispersion as well as for the waveguide case. For a given sequence

$$t_{\min}^{\text{plane wave}} > t_{\min}^{\text{waveguide}}. \tag{12}$$

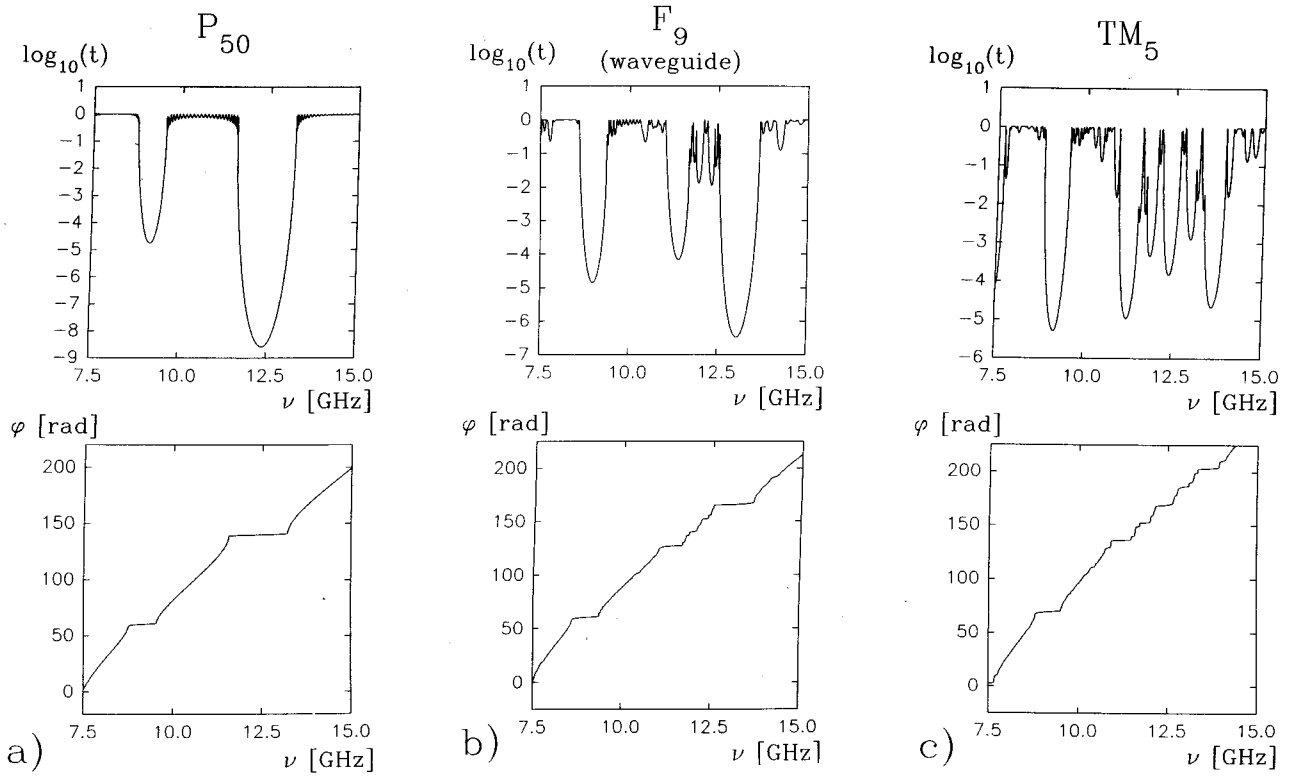


FIG. 3. Transmission spectra for the waveguide dispersion of the elements shown in Fig. 2. Due to the altered dispersion relation the λ/4 condition Eq. (9) does not hold.

Although the Thue-Morse system $T_5^{\mathrm{TM}}$ is actually longer than the periodic and Fibonacci systems and the gaps become deeper with increasing system length (see below), relation (11) is observed. The more ordered the system is, the more easily standing waves can build up in and between the layers and more clearly the coherent interference pattern emerges. In this sense the Fibonacci sequence is more ordered than the Thue-Morse sequence.

In order to point out this situation, let us consider a given sequence as one single layer of thickness $L$ having an effective wave vector $k_{\mathrm{eff}}$. The transmission is very small in the gaps and decreases with increasing system length. Above a given thickness we can neglect multiple reflections between the front and the backside of the sequence. With $|a|=|\exp(-ik_{\mathrm{eff}}L)|\ll 1$ Eq. (3) may be written as $S_{21}=\exp(-i\varphi)=(1-r_{\mathrm{eff}}^2)\exp(-ik_{\mathrm{eff}}L)$ and thus in the gaps

$$\ln(t_{\mathrm{gap}})=\mathrm{Im}[k_{\mathrm{eff}}]L+\ln|1-r_{\mathrm{eff}}^2|, \tag{13}$$

$$\varphi_{\mathrm{gap}} \bmod 2\pi=\mathrm{Re}[k_{\mathrm{eff}}]L+\varphi_0, \tag{14}$$

where $\varphi_0$ denotes the phase shift due to the transitions at the front and the back of the sequence ($\tan\varphi_0=\mathrm{Im}[1-r_{\mathrm{eff}}^2]/\mathrm{Re}[1-r_{\mathrm{eff}}^2]$). Measured phase and amplitude yield real and imaginary parts of the effective complex wave number of the system. This is shown in Fig. 4 for the Fibonacci sequence. For the calculation of the phase, multiples of $2\pi$ are added according to the number $n$ of $\frac{3}{4}\lambda$ layers: $\varphi=\varphi_{\mathrm{calc}}+\mathrm{Int}[n\frac{3}{4}+\frac{1}{2}]2\pi$ (in the periodic case, for example, the phase difference between two consecutive elements is exactly $\frac{3}{2}\pi$). In fact, the above linear relations (13) and (14) are observed at the gap frequencies. So the assumption of a complex effective wave number independent of $L$ is correct. In the gap regions the phase variation $d\varphi/d\omega$ is small (see Figs. 2 and 3) and below we shall show that the real part of $k_{\mathrm{eff}}$ does not contribute for long systems. The negative imaginary part causes an exponential decay of the transmitted amplitude with increasing system length. For an infinite system $t$ becomes zero and a completely forbidden band gap is obtained. In the absence of dissipation (lossless material) the decay [Eq. (13)] is caused by a distributed quasitotal reflection along the system. This situation is similar to the exponential decay of evanescent modes in undersized

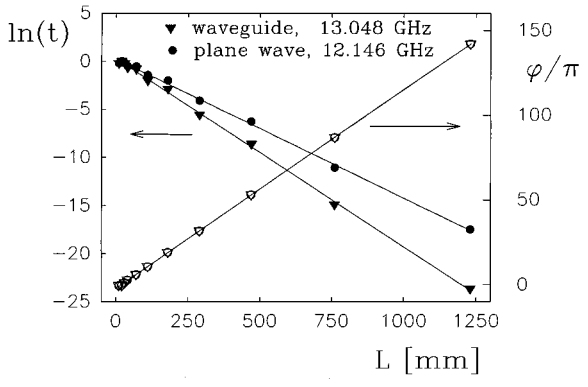


FIG. 4. Amplitude (filled symbols, left $y$ axis) and phase (open symbols, right $y$ axis) in the gaps of the Fibonacci sequence vs system length (circles, plane-wave dispersion; triangles, waveguide dispersion). The linear dependence shows that the propagation can be described by a complex effective wave number [Eqs. (13) and (14)].

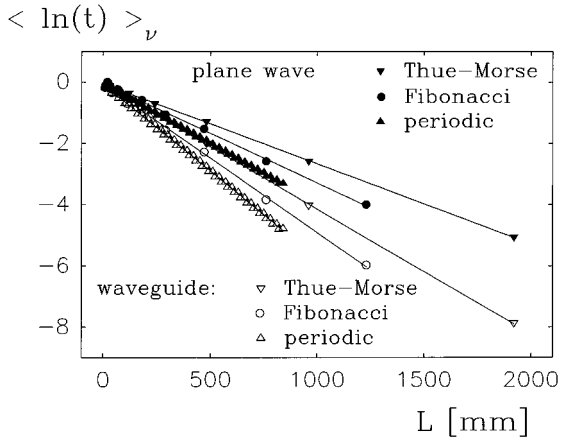


FIG. 5. Frequency-averaged amplitude of the transmission coefficient [see Eq. (15)] in semilogarithmic plot vs system length. For the values of the decay lengths see Table I.

waveguides, where $k$ is a pure imaginary quantity [Eq. (1) with $(\nu_c/\nu)^2 > \varepsilon\mu$] [15–17]. However, in an undersized waveguide the local and the effective wave number equal each other, i.e., the system is homogeneous in the direction of propagation. In our case the spectra are calculated by the superposition of transmitted and reflected waves of single layers $A$ and $B$ with the above specified local $k$ numbers [Eq. (1)]. Both the exponential decay and the small phase variation are the result of multiple reflections of oscillating propagating waves, i.e., an interference effect. For this reason the phase increases with increasing system length, i.e., $\mathrm{Re}[k_{\mathrm{eff}}] \neq 0$, in contrast to evanescent waveguide modes.

In order to measure the degree of order, i.e., the strength of coherent interference, we compare the decay lengths $\tilde{\alpha} = -1/\mathrm{Im}[k_{\mathrm{eff}}]$ of the sequences and average over the whole frequency period from 7.5 to 15 GHz. Thus Eq. (13) becomes

$$\langle \ln(t) \rangle_\nu = -\frac{1}{\alpha} L + \text{const.} \tag{15}$$

Although Eq. (15) resembles the definition of the localization length $\xi$ (the constant is of the order of 0; see Fig. 5), our $\alpha$ values should not be confused with this quantity. In order to determine localization lengths, only frequencies outside the forbidden gap of the periodic systems have to be taken (and thus in the periodic case $\alpha = \xi = \infty$, i.e., there is no localization). Here we are interested in the strength of coherent interference and thus also in the gap region.

The constant slope in Fig. 5 proves that $\mathrm{Im}[k_{\mathrm{eff}}]$ is in fact independent of $L$ for sufficient large system sizes. Inside the gaps Eq. (15) holds without frequency averaging (see Fig. 4). Outside the gaps $t$ is close to unity and does not contribute to $\langle \ln(t) \rangle_\nu$. The deeper the gaps become [small $t$, large $-\ln(t)$], the more $\alpha$ should decrease [Eq. (15)]. Thus the averaged decay length $\alpha$ is sensitive to both the number and the depth of gaps. From Eq. (11) we expect to observe the slowest decay for the Thue-Morse system. In fact, we obtain (Fig. 5 and Table I)

$$(\alpha^{\text{Thue-Morse}} > \alpha^{\text{Fibonacci}} > \alpha^{\text{periodic}})_{\text{plane wave}} > (\alpha^{\text{Thue-Morse}} > \alpha^{\text{Fibonacci}} > \alpha^{\text{periodic}})_{\text{waveguide}} . \tag{16}$$

Table I also shows the respective decay lengths in units of a building block: $3\lambda_{\mathrm{PW}}/4 = \sqrt{\varepsilon_a} d_a = d_b$. The largest decay length corresponds to 19 building blocks (plane wave, Thue-Morse) and the smallest to about 9 building blocks (waveguide, periodic).

The negative interference due to multiple reflection inside and between the layers is most effective for a periodic system creating very deep gaps and thus a very small decay length. Increasing disorder disturbs the coherent interference, the gaps become more shallow, and the decay length increases. The decay lengths of the waveguide systems are smaller due to additional gaps caused by the altered dispersion relation (Figs. 2 and 3). However, one should keep in mind that the waveguide case does not correspond to a quarter-wavelength system (as we shall see below, a waveguide $\lambda/4$ system exhibits $\alpha$ values similar to those of the plane-wave case). Carpena *et al.* [18] used $\langle t^2 \rangle_\nu$ and thus they got the inverse relation for the decay lengths. But in this case mainly frequencies outside the gaps ($0 \ll t \simeq 1$) contribute to the average decay length ($\langle t^2 \rangle$ is a measure for the number of gaps; the depth gives no contribution when the system is sufficiently long).

### B. Barrier traverse: Delay times and velocities

Periodic and quasiperiodic dielectric sequences form a potential barrier in which the wave decays exponentially. In addition, the frequency variation is very small and thus there is no ordinary propagating mode. The question of how much time a wave or a particle requires to traverse a barrier has attracted much interest (see [19–21] and references cited therein), especially since superluminal velocities have been observed in undersized waveguides [15–17,22] or in periodic dielectric heterostructures [23,24]. It is still an open question which definition of the delay time corresponds to the tunneling time of a photon or of a wave packet [19,20,25], i.e., the time for the traverse of an evanescent region. For example, the usual definition of the energy velocity $v_E = |P|/w$ via the time-averaged Poynting vector

TABLE I. Decay lengths of different systems [see Fig. 5 and Eq. (15)]. The lengths in units of a 3/4-wavelength building block $3\lambda/4 = \sqrt{\varepsilon_a} d_a$ refer to the center wavelength of the spectra.

| | Plane wave | | | Waveguide | | |
|---|---|---|---|---|---|---|
| Decay length | Thue-Morse | Fibonacci | Periodic | Thue-Morse | Fibonacci | Periodic |
| $\alpha$ (mm) | 383 | 308 | 256 | 246 | 207 | 176 |
| $\alpha/(3\lambda/4)$ | 19.15 | 15.40 | 12.80 | 12.30 | 10.35 | 8.80 |

$\overline{P}=\mathrm{Re}[\overline{E}\times\overline{H^*}]$ and energy density $w$ does only apply for the propagation in a medium without any reflections at interfaces. At an interface incoming $(E^i,H^i)$ and reflected $(rE^i,-rH^i)$ waves are superposed and the effective Poynting vector becomes $P^{\mathrm{eff}}=P^i+P^{\mathrm{refl}}=(1-|r|^2)P^i$ (note that the sign of $P^i$ and $P^{\mathrm{refl}}$ differs) and $w^{\mathrm{eff}}=(1+|r|^2)w_i$. A calculation on the basis of the total electric and magnetic fields would average the velocities of incoming and reflected wave:

$$v_E^{\mathrm{eff}}=\frac{1-|r|^2}{1+|r|^2}v_E^i=\frac{v_E^i-|r|^2v_E^{\mathrm{refl}}}{1+|r|^2}. \tag{17}$$

This value is smaller than $v_E^i$, the energy velocity of the wave propagating forward. For example, at the open end of a coaxial cable nearly the whole wave is reflected ($r\to 1$ for low frequencies) since $E\to 2E^i$ and $H\to 0$. So $v_E^{\mathrm{eff}}$ becomes very small, but of course it cannot be assigned to the small amount of energy radiated from the open end into space. The exponential decay associated with the tunneling problem corresponds to a distributed reflection (see above). Inside the barrier the incoming and all the reflected waves are superposed. Thus a calculation of the local field distribution in the barrier cannot yield the energy velocity of the transmitted wave (taking the Poynting vector behind the barrier would yield the normal energy velocity in free space or in a waveguide, respectively, which does not characterize the barrier). The waves before and behind the barrier have to be compared, i.e., in the frequency domain via transmission coefficients or via an equivalent Fourier transform into the time domain.

In general, the propagation of a wave packet in a medium without dispersion can be characterized by its phase time (or group delay)

$$\tau_\varphi=d\varphi/d\omega, \tag{18}$$

where $\varphi=\mathrm{Re}[k]L$. Later we shall be able to seperate boundary effects. *A priori* this is impossible and we have to characterize the whole barrier by rewriting Eq. (14) as $\varphi_{\mathrm{gap}}=k_rL$, with $k_r=\mathrm{Re}[k_{\mathrm{eff}}]+k_b$ ($k_b=\varphi_0/L$ is the contribution of the boundaries at the front and at the back). The complex wave vector associated with the tunneling problem usually shows a strong dispersion $k(\omega)$. This may cause reshaping of the incoming wave packet, an effect that depends on its frequency bandwidth, and thus alters the movement of the center of gravity or of the maximum. The phase time approach is correct as long as two assumptions are fulfilled: (i) The disperion $\omega(k_r)$ can be expanded around the center value of the wave packet $k_0$, i.e., $\omega(k_r)=\omega_0+(d\omega/dk_r)_0(k_r-k_0)+\ldots$, and the amplitude of the contributing frequencies is fairly sharply peaked around $k_0$ so that higher terms of the above Taylor expansion can be neglected [26] and (ii) the frequency dependence of the imaginary part of the wave vector is sufficiently small so that the amplitude of the frequency components $t=\exp\{\mathrm{Im}[k(\omega)]L\}$ is scarcely affected (see below). In this case the pulse travels along undistorted in shape with the group velocity

$$v_{\mathrm{gr}}=\left.\frac{d\omega}{dk_r}\right|_0=\frac{L}{\tau_\varphi} \tag{19}$$

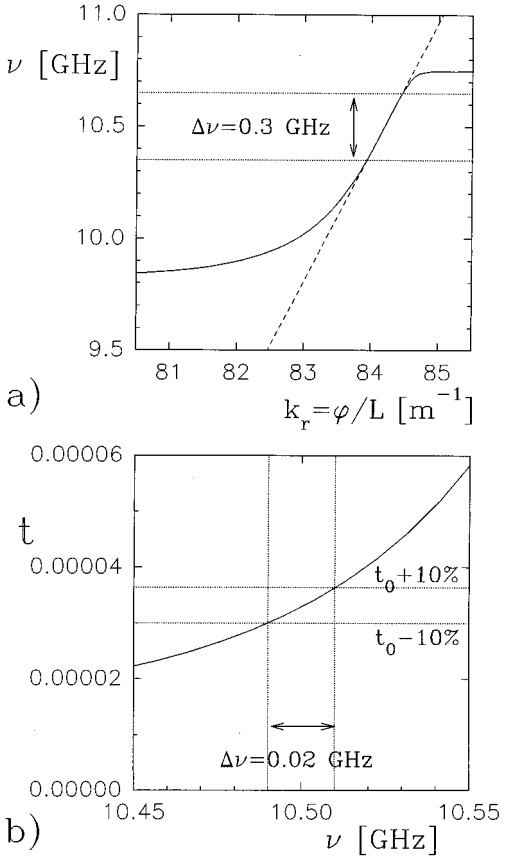


FIG. 6. (a) Plane-wave dispersion $\nu(k_r)$ for the Fibonacci element $F_9$ in the gap region. The dashed line shows the validity of the first-order Tayler expansion at 10.5 GHz. (b) Amplitude of the transmission coefficient vs frequency near 10.5 GHz, showing the dispersion due to the imaginary part of the wave number.

As long as the pulse remains undistorted ''the transport of energy occurs with the group velocity'' [26]. The group velocity describes the propagation of the center of gravity and entirely characterizes the transmitted wave packet. At an optical resonance frequency in the range of anomalous dispersion, for example, the above conditions may not hold [26]. Reshaping occurs and calculated negative or superluminal group velocities have no physical meaning. Using undersized waveguides, Enders and Nimtz [15] have pointed out that for narrow-band frequency limited wave packets ($|\Delta k|L<1$) traversing opaque ($|k|L>1$) evanescent regions the pulse reshaping can be neglected. The experiments in both the time and the frequency domain [Eq. (19) or via Fourier transform] yielded superluminal velocities [15,16,22,27]. In order to check whether the phase time approach is correct for the systems studied we display the plane-wave dispersion $\nu(k_r)$ for the Fibonacci element $F_9$ near 10.5 GHz, where the frequency variation reaches its maximum value [Fig. 6(a)]. In a frequency band of about 0.3 GHz the abovementioned linear expansion is valid. Due to the frequency dependence of $\mathrm{Im}[k]$ the bandwidth has to be restricted to 0.02 GHz in order to ensure a maximum deviation of $\pm 10\%$ between the amplitudes [see Fig. 6(b)]. Thus the phase time approach is correct for a bandwidth of $\Delta\nu/\nu=0.19\%$. For the periodic structure $P_{50}$ the maximum of $v_{\mathrm{gr}}$ and the minimum of $t$ occur at the same frequency and

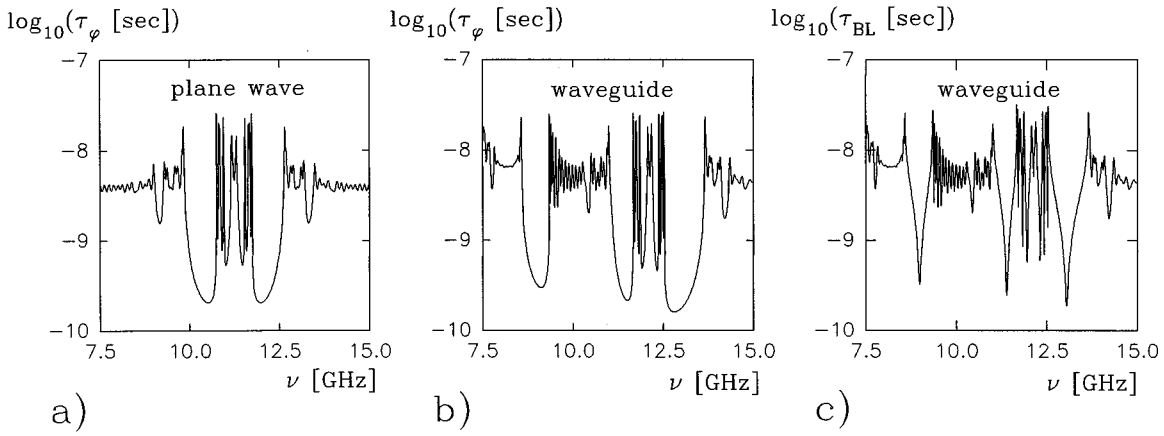


FIG. 7. (a) and (b) Phase time and (c) optical analogue of the Büttiker-Landauer tunneling time [Eq. (20)] vs frequency in a semilogarithmic plot for the Fibonacci element $F_9$.

a bandwidth of 0.175 GHz, i.e., $\Delta\nu/\nu=1.56\%$ is possible. In the following we restrict ourselfs to band limited wave packets showing no reshaping effects so that the group velocity equals the energy velocity. Due to the finite bandwidth, the width of the wave packet in space is large. For the rms deviation of the average value $\Delta x\Delta k\geqslant 0.5$ holds [26]. For the plane-wave dispersion ($\Delta k=\Delta\omega/c$ outside the barrier) of the Fibonacci element $F_9$ we obtain $\Delta x\geqslant 1.19$ m, compared to a barrier length of 0.76 m ($\Delta x\geqslant 0.136$ m for $P_{50}$). Moreover, the finite frequency range corresponds to an infinite extension in space or in time. The discussion whether such wave packets model the wave function of single photons or electrons or whether they might be interpreted as signals lies beyond the scope of this paper and we refer to Ref. [27].

Another approach for the barrier traverse is the optical analog of the Büttiker-Landauer tunneling time [28,29], rewritten for electromagnetic waves and based on Faraday rotation [30]

$$\tau_{\mathrm{BL}}=\sqrt{\left(\tau_\varphi+\frac{\mathrm{Im}[S_{11}+S_{22}]}{4\omega}\right)^2+\left(\frac{d\ln t}{d\omega}+\frac{\mathrm{Re}[S_{11}+S_{22}]}{4\omega}\right)^2}. \tag{20}$$

The reflection coefficients $S_{11}$ and $S_{22}$ take into account the particular features of the shape of the barrier (for a symmetric one $S_{11}=S_{22}$) and become important at low frequencies and/or for short barriers [31]. For photons, the term in the first set of parentheses in Eq. (20) is proportional to the Faraday rotation or the density of optical modes, while the term in the second set of parentheses is proportional to the degree of ellipticity or to the radius of localization [30]. In contrast to the phase time, for $\tau_{\mathrm{BL}}$ the change of both the phase and the amplitude has to be taken into account. Note that even for very-narrow-band wave packets showing no reshaping effects in the time domain, the term $d\ln t/d\omega$ in Eq. (20) yields a time that is, in general, larger than the phase time. In this case $\tau_{\mathrm{BL}}$ does not correspond either to the delay of the center of gravity or to the delay of the maximum, and a physical interpretation becomes difficult.

In order to discuss the behavior of the periodic and quasiperiodic sequences we start with $\tau_\varphi$ [Eq. (18)]. In the gap regions the phase changes only slowly with frequency (Figs. 2 and 3) and the phase time becomes small [see Figs. 7(a) and 7(b)]. Above a certain system size, $\tau_\varphi$ becomes quasi independent of the length, i.e., it alternates between two distinct values $\tau_1$ and $\tau_2$ (see Fig. 8): for the plane-wave case, for example, between $\tau_1=2\times10^{-10}$ s and $\tau_2=1.33\times10^{-10}$ s (periodic), between $\tau_1=2.04\times10^{-10}$ s and $\tau_2=3.34\times10^{-10}$ s (Fibonacci), and between $\tau_1=2.38\times10^{-10}$ s and $\tau_2=3.28\times10^{-10}$ s (Thue-Morse). For the waveguide similar values are obtained (see Table II). Thus, increasing disorder enhances the minimum phase time. The fact that $(\tau_\varphi)_{\min}$ alternates between two distinct values is due to an additional phase variation in every second element. For the periodic case, for example, every odd element is obtained from the previous even one by adding a nonreflecting air layer. This results in an additional phase $\varphi_+=k_bd_b$, and thus in the plane-wave case $d\varphi_+/d\omega=d_b/c=\frac{2}{3}\times10^{-10}$ s $=\tau_1-\tau_2$ (see above). Adding the next layer $A$ reestablishes the starting point, i.e., the sequence is terminated by a reflecting layer. Considering a sequence as an effective system, $\varphi_{\mathrm{gap}}=\mathrm{Re}[k_{\mathrm{eff}}]L+\varphi_0$ [see Eq. (14)]. $\varphi_0$ describes the phase shift due to the transitions at the front and the back of the system and thus also comprises the above variation of $\varphi_+$.

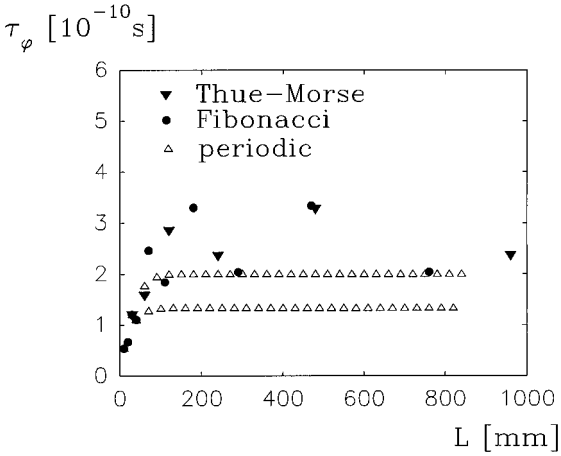


FIG. 8. Minimum phase times vs system length for the plane-wave case. Similar curves are obtained for the waveguide dispersion.

TABLE II. Minimum values of the phase time $\tau_\varphi$ and of the optical analog of the Büttiker-Landauer tunneling time $\tau_{BL}$ [see Eq. (20)]. These values are obtained in the gaps. Above a given system length the $\tau$ values of a sequence alternate between two values; see Fig. 8.

| | Plane wave | | Waveguide | |
|---|---|---|---|---|
| Sequence | $(\tau_\varphi)_{min}$ ($10^{-10}$ s) | $(\tau_{BL})_{min}$ ($10^{-10}$ s) | $(\tau_\varphi)_{min}$ ($10^{-10}$ s) | $(\tau_{BL})_{min}$ ($10^{-10}$ s) |
| periodic $P_{50}$ | 1.334 | 1.337 | 1.195 | 1.226 |
| $P_{49}$ | 2.001 | 2.001 | 1.984 | 2.023 |
| Fibonacci $F_9$ | 2.041 | 2.281 | 1.599 | 1.881 |
| $F_8$ | 3.341 | 3.403 | 2.742 | 2.775 |
| Thue-Morse $T_5$ | 2.378 | 2.423 | 1.808 | 1.899 |
| $T_4$ | 3.284 | 3.285 | 3.433 | 3.432 |

Obviously the real part of the effective wave number is constant (see Fig. 8) and thus

$$(\tau_\varphi)_{gap}=\frac{d\varphi_0}{d\omega},$$

i.e., only a nonoscillating effective evanescent mode exists and the phase variation of $S_{21}$ is caused by the transitions and is independent of the system length as in undersized waveguides [17] (the difference between real and effective evanescent modes has already been pointed out above). In the gap regions the wave propagation is determined by the imaginary part of $k_{eff}$, which is independent of $L$ [see above and Eqs. (13) and (14)]. In contrast, the phase time becomes very large at the edges of the gaps. This may be interpreted as a longer interaction and is caused by a shift of gap states towards the edges. The density of states is [31]

$$N(\nu)=\left(\frac{\partial\varphi}{\partial\nu}+\frac{\mathrm{Im}[S_{11}+S_{22}]}{4\nu}\right)\frac{1}{h\pi L} \tag{21}$$

($L$ is the system length and $h$ is the Planck constant). We do not display the data since the shape of the curve resembles that of the phase time $\tau_\varphi$ (Fig. 7). Even in the gap regions, where $d\varphi/d\nu$ becomes small, the contribution of the term $\mathrm{Im}[S_{11}+S_{22}]/4\nu$ is smaller than 2%. Outside the gaps it can be neglected. Thus the phase time is proportional to the density of states of electromagnetic modes in the system. It reproduces the characteristic features of the one-dimensional system, i.e., $d\varphi/d\omega$ shows the Van Hove singularities at the band edges [32]. In the forbidden gap the density of states becomes very small (it would become zero for an infinite system) and so does $d\varphi/d\omega$.

Figure 7(c) displays the Büttiker-Landauer time $\tau_{BL}$ [Eq. (20)] for the waveguide dispersion of the Fibonacci element $F_9$. Compared to the $\tau_\varphi$ curve [Fig. 7(b)], the width of the $\tau$ gaps is decreased; however, similar minimum values are observed at the center frequencies of the gaps. The same holds for the plane-wave disperion. A narrow-band frequency limited wave packet with a center frequency at the gap minimum will not be distorted and its barrier traverse time is given by $\tau_\varphi\simeq\tau_{BL}$. Using the definition of $\tau_{BL}$ only demands a more restricted frequency range to obtain low delay times for all frequency components. In Table II the minimum values of $\tau_{BL}$ according to Eq. (20) are listed. It is easy to understand why the values are close to those of $\tau_\varphi$. At the gap frequency where ln$t$ is a minimum $d\ln t/d\omega=0$ and thus Eq. (20) becomes ($|S_{11}|,|S_{22}|\leqslant 1$)

$$(\tau_{BL})_{gap}=\sqrt{\tau_\varphi^2+\tau_\varphi\mathrm{Im}[S_{11}+S_{22}]/2\omega_{gap}+\left(\frac{|S_{11}+S_{22}|}{4\omega_{gap}}\right)^2} \tag{22}$$

$$\leqslant\tau_\varphi+\frac{1}{2\omega_{gap}}, \tag{23}$$

with $(2\omega_{gap})^{-1}\ll(\tau_\varphi)_{gap}$ (see Table II). For the waveguide dispersion the Fibonacci element $F_9$, for example, has a minimum at $\nu_{gap}=13.05$ GHz (see Fig. 3) and $(\tau_\varphi)_{min}=1.599\times10^{-10}$ s $\gg 6.1\times10^{-12}=1/2\omega_{gap}$. The minimum of $\tau_\varphi$ is located at $\nu_0=12.8$ GHz (see Fig. 7). However, the frequency difference is small and $\tau_\varphi(\nu_{gap})\simeq(\tau_\varphi)_{min}$ and thus also $(\tau_{BL})_{gap}\simeq(\tau_{BL})_{min}$, which is listed in Table II. In the middle of the gaps the Büttiker-Landauer time is just sligthly larger than the phase time, which can be considered as the barrier traverse time. For both the plane-wave and the waveguide dispersion $(\tau_\varphi)_{gap}\simeq(\tau_{BL})_{gap}$ and these times are independent of the length for larger system sizes. Increasing disorder, i.e., changing from spatial periodicity to quasiperiodic long-range order, results in higher $\tau$ values.

In an undersized waveguide [Eq. (1) with $(\nu_c/\nu)^2>\varepsilon\mu$] the Büttiker-Landauer time differs from $\tau_\varphi$. The term $d\ln t/d\omega$ gives a contribution proportional to the length of the system. When the system is sufficiently long we can neglect multiple reflections and thus Eq. (13) yields

$$\frac{d\ln t}{d\omega}=\frac{\varepsilon\mu}{\sqrt{(\nu_c/\nu)^2-\varepsilon\mu}}\frac{L}{c}$$

(assuming lossless material, i.e., $\varepsilon$ and $\mu$ are real quantities only). Thus $\tau_\varphi<\tau_{BL}$, whereas for our quasiperiodic structures $\tau_\varphi\simeq\tau_{BL}$.

Since the gap times of periodic and quasiperiodic structures are independent of $L$, superluminal velocities $L/\tau$ are obtained while at the edges very small values are observed (for a measurement of $v_{gr}>c$ in periodic systems see Ref. [24]). The group velocity $v_{gr}=L/\tau_\varphi$ is displayed in Fig. 9. Taking $L/\tau_{BL}$ would yield nearly the same maximum values, but peaks of a reduced width. As a consequence of the $\tau$ plateaus shown in Fig. 8, the gap values of the group velocities increase with increasing system length (see Fig. 10). The

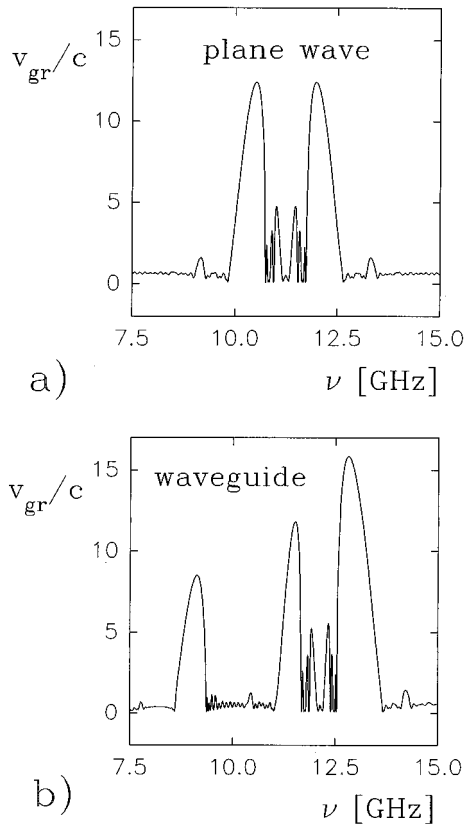


FIG. 9. Normalized group velocity vs frequency for the Fibonacci element $F_9$.

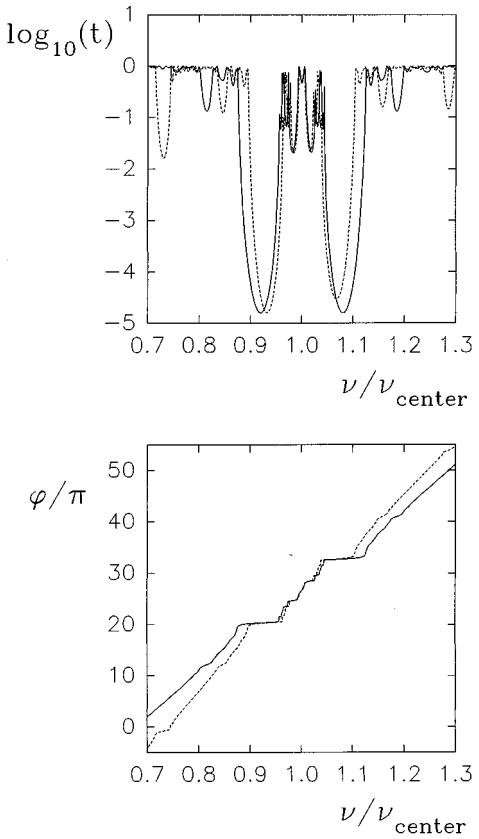


FIG. 11. Transmission spectrum of the Fibonacci element $F_9$ vs normalized frequency (3/4λ systems). Solid lines, plane wave; dashed lines, waveguide. Between $20.5\pi$ and $33.5\pi$ phase plateaus appear in steps of $\pi$.

most ordered periodic structure exhibits the highest values. As we have already pointed out, sufficient narrow-band wave packets centered around a gap frequency will not show reshaping effects. The transmitted wave packet will exhibit a much smaller amplitude, but the same shape, and is characterized by a superluminal group velocity.

Also in waveguide experiments with evanescent modes superluminal velocities have been observed [15,16]. However, in our case the small phase change of the transmission coefficient is the result of multiple reflections of propagating waves, i.e., an interference effect, resulting in a quasitotal reflection. Thus real evanescent modes are not a necessary condition for superluminal group velocities; quasitotal reflection is sufficient.

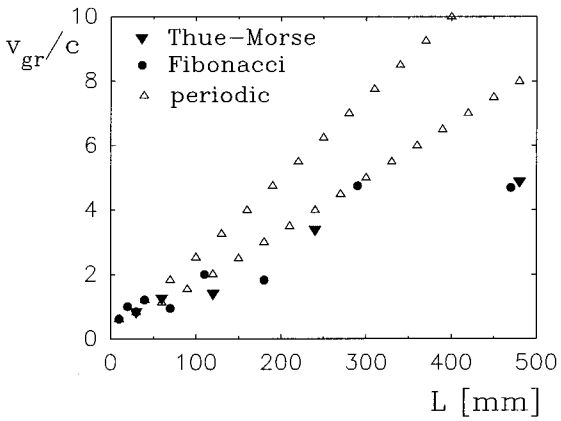


FIG. 10. Maximum values of the group velocity vs system length for the plane-wave case.

### C. Scaling properties

Until now we have compared the behavior of plane-wave and waveguide systems assembled from the same two building blocks. Due to the different dispersion relations, only the plane-wave systems were 3/4-wavelength systems. So let us compare two Fibonacci systems that fulfill the 3/4-wavelength condition for the plane-wave and for the waveguide case, respectively. We keep the above specified parameters for the plane-wave case. For the waveguide we only change the permittivity of layer $A$ from $\varepsilon_a = 4$ to $\varepsilon_a = 3.238$. Thus Eq. (9) is fulfilled; the waveguide center frequency is $\nu_{\text{center}} = 13.016$ GHz instead of 11.242 GHz. In Fig. 11 the $F_9$ spectra are shown as a function of the normalized frequency $\nu/\nu_{\text{center}}$. Due to the altered dispersion relation, the waveguide spectra lose their symmetry far from $\nu_{\text{center}}$; however, it is preserved near $\nu_{\text{center}}$ (this is also true for the periodic and the Thue-Morse sequences, which are not shown). Thus quarter-wavelength systems show in principle a similar behavior for both dispersion relations. In particular, nearly the same decay lengths (Fig. 5), phase times (Figs. 7 and 8), and thus also density of states [Eq. (21)] and group velocities should be obtained for plane-wave and waveguide systems. In the frequency range between the two

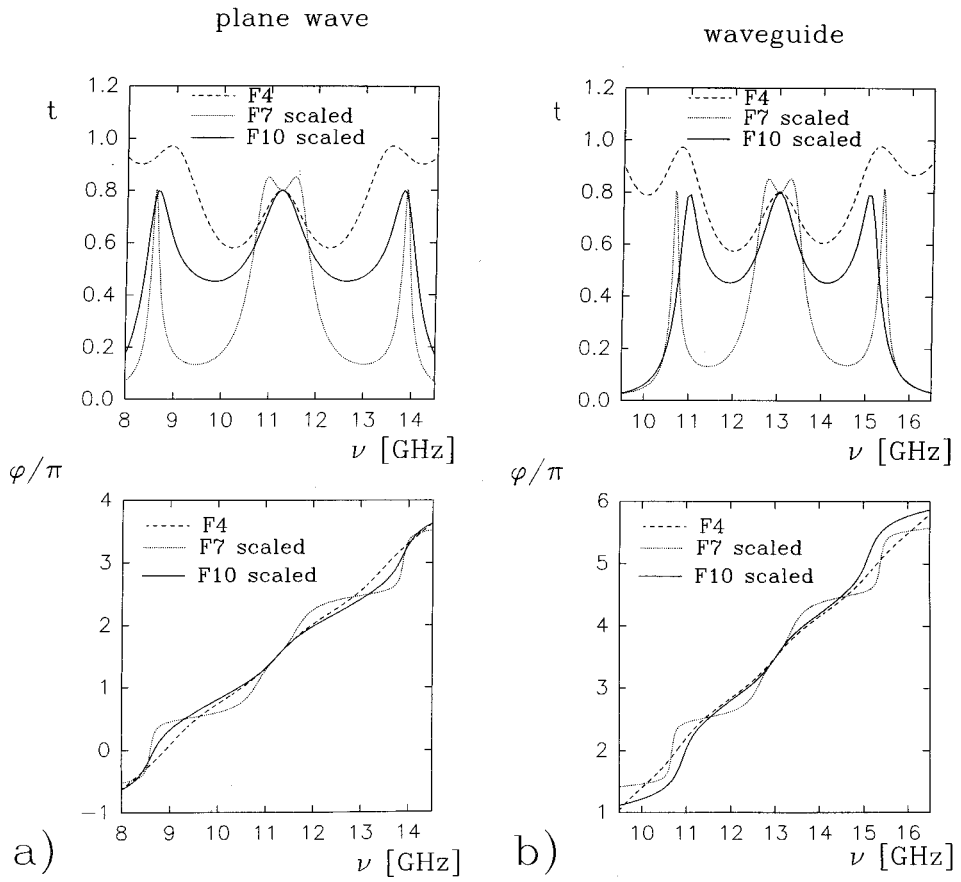


FIG. 12. Fibonacci spectrum $F_4$ as well as scaled spectra $F_7$ and $F_{10}$ vs frequency for (a) plane wave dispersion and (b) waveguide dispersion (3/4 λ systems).

main gaps the phase plateaus appear in steps of $\pi$ at values of $(n+1/2)\pi$. (In Ref. [33] the gaps are located at integer values of $\pi$; however, periodic boundary conditions have been used for the calculation.)

At $\nu_{\text{center}}$ the transmission matrices of $(2n+1)\times$ λ/4 layers have a periodicity of 6, i.e., $T_{i+6}=T_i$ [9]. The first two elements of the Fibonacci sequence are the single-layer matrices $T_0=T_b$ (air) and $T_1=T_a$ (dielectric). From Eqs. (3), (4), and (6) with $a=\exp(-ikd)=i(-1)^{n+1}$ (in our case $n=1$) we obtain

$$T_0=i(-1)^n\begin{pmatrix}-1 & 0\\ 0 & 1\end{pmatrix},\quad T_1=i(-1)^n\alpha\begin{pmatrix}-1 & \beta\\ -\beta & 1\end{pmatrix},$$

where $\alpha=(1+r^2)/(1-r^2)$ and $\beta=2r/(1+r^2)$. With $\alpha^2(1-\beta^2)=1$, Eq. (8) yields, for the next elements,

$$T_2=-\alpha\begin{pmatrix}1 & \beta\\ \beta & 1\end{pmatrix},$$

$$T_3=i(-1)^{n+1}\alpha^2\begin{pmatrix}-(1+\beta^2) & 2\beta\\ -2\beta & (1+\beta^2)\end{pmatrix},$$

$$T_4=T_1,\quad T_5=\alpha\begin{pmatrix}1 & -\beta\\ -\beta & 1\end{pmatrix}.$$

Since $T_6=T_5T_4=T_0$ and $T_7=T_6T_5=T_1$ the period of 6 is obvious. The amplitude of the transmission coefficients $t_i=(1/T_{22})_i$ of the first six elements are thus $t_0=1$, $t_1=t_2=t_4=t_5=1/\alpha$, and $t_3=\alpha^{-2}/(1+\beta^2)=(1-\beta^2)/(1+\beta^2)$. Of course, this result does not depend on the dispersion relation (1). A periodicity of 3, i.e., $t_i=t_{i+3}$, holds for $i=1$ mod3 and $i=2$ mod3, but is only approximately valid for $i=0$ mod3 in the case of weak reflection $(\varepsilon_a/\varepsilon_b\simeq 1\Rightarrow r\ll 1\Rightarrow\alpha\simeq 1,\ \beta\simeq 0)$.

Now let us check the so-called scaling relation [9,34,35], which has been interpreted as a sign for quasilocalization of the states. The transmission coefficient should exhibit a self-similar behavior around the center frequency with $t_i(\nu_{\text{scaled}})\simeq t_{i+3}(\nu)$, i.e., replacing the frequency axis of a spectrum by $\nu_{\text{scaled}}=(\nu-\nu_{\text{center}})f+\nu_{\text{center}}$ should yield the spectrum of a higher element. The (slightly-frequency-dependent) scaling factor $f$ is [34,35] $f=\sqrt{1+4(1+I)^2}+2(1+I)$, with $I=\frac{1}{4}\sin^2(k_ad_a)\sin^2(k_bd_b)(\sqrt{\varepsilon_a/\varepsilon_b}-\sqrt{\varepsilon_b/\varepsilon_a})^2$. For the center frequency of the plane-wave spectrum $I=0.5625$ and thus $f=6.4061$; for the waveguide $I=0.386\,708$ and thus $f=5.7216$. Since the periodicity of 3 does not hold for $i=0$ mod3, we chose the spectra $F_4$, $F_7$, and $F_{10}$ (see Fig. 12). The plane-wave and the waveguide spectra show the same behavior. The $F_4$ and $F_{10}$ curves resemble each other near $\nu_{\text{center}}$, however, $F_7$ differs. Once again, the periodicity of 6, i.e., the scaling $t_i(\nu_{\text{scaled}})\simeq t_{i+6}(\nu)$ with scaling factor $f^2$, is fulfilled, whereas the numerically found scaling of 3 (see Ref. [35]) does not hold in general.

## IV. CONCLUSION

In the photonic band gaps periodic and quasiperiodic multilayer systems can be described by a complex effective

wave number. Its negative imaginary part causes an exponential decay of the transmission coefficient with increasing system length: $t_{\mathrm{gap}}=\exp(\mathrm{Im}[k_{\mathrm{eff}}]L)$. Since only lossless materials have been considered, the decay corresponds to a distributed quasitotal reflection. The phase $\varphi_{\mathrm{gap}}=\mathrm{Re}[k_{\mathrm{eff}}]L+\varphi_0$ increases with increasing system length; however, the phase times $\tau_\varphi=d\varphi/d\omega$ are independent of $L$ for larger system sizes, i.e., $d\mathrm{Re}[k_{\mathrm{eff}}]/d\omega=0$. $\tau_\varphi$ only alternates between two distinct values and roughly equals the Büttiker-Landauer tunneling time. Thus superluminal group velocities are obtained, characterizing the propagation of very-narrow-band wave packets.

The observed behavior calls to mind evanescent modes in undersized waveguides, where $k$ is a pure imaginary quantity. However, a multilayer system is not homogeneous in the direction of propagation due to different local wave numbers. The effective wave number results from multiple reflections of oscillating propagating waves, i.e., from an interference effect. For this reason the phase increases with increasing system length, i.e., $\mathrm{Re}[k_{\mathrm{eff}}]\neq 0$, in contrast to evanescent waveguide modes.

For both the plane-wave and the waveguide dispersion the most ordered structures exhibit the most effective coherent interference and thus the deepest gaps in the transmission spectra as well as the smallest decay length $\alpha=-1/\langle\mathrm{Im}[k_{\mathrm{eff}}]\rangle_\nu$. Thus the Thue-Morse sequence is less ordered than the Fibonacci one, which in turn is, of course, less ordered than the periodic system. Increasing disorder enhances the phase times, the Büttiker-Landauer times, and the density of states in the gap regions. The group velocities become smaller but remain superluminal.

Arranging the building blocks of a plane-wave quarter-wavelength system in a waveguide breaks the $\lambda/4$ condition due to the altered dispersion relation. The gaps become deeper, additional ones appear, and the averaged decay lengths decrease. Normalizing the frequency axis with regard to the center frequency, the spectra of $\lambda/4$ systems are similar for both the plane-wave and the waveguide dispersion. The Fibonacci scaling relation has been checked for both dispersion relations. It holds for a periodicity of 6, whereas the claimed [9,34,35] periodicity of 3 has been found to be invalid in general.

## ACKNOWLEDGMENTS

We gratefully acknowledge fruitful discussions with W. Heitmann and financial support by the Graduiertenkolleg Scientific Computing, University of Cologne.

[1] M. Kohmoto and C. Tang, Phys. Rev. B **34**, 2041 (1986).
[2] F. Nori and J. P. Rodriguez, Phys. Rev. B **34**, 2207 (1986).
[3] H. Böttger and G. Kasner, Phys. Status Solidi B **162**, 489 (1990).
[4] L. N. Gumen and O. V. Usatenko, Phys. Status Solidi B **162**, 387 (1990).
[5] C. L. Roy and A. Khan, Solid State Commun. **92**, 241 (1994).
[6] P. K. Ghosh, Phys. Lett. A **139**, 275 (1989).
[7] D. Badalian, V. Gasparian, R. Abramian, A. Khacahatrian, and U. Gummich, Physica B **226**, 385 (1996).
[8] M. Kohmoto, B. Sutherland, and K. Iguchi, Phys. Rev. Lett. **58**, 2436 (1987).
[9] W. Gellermann, M. Kohmoto, B. Sutherland, and P. C. Taylor, Phys. Rev. Lett. **72**, 633 (1994).
[10] S. John, Phys. Today **44**(5), 32 (1991).
[11] A. Rost, *Messung Dielektrischer Stoffeigenschaften* (Vieweg, Braunschweig, 1978), pp. 112 and 145–146.
[12] A. M. Nicolson and G. F. Ross, IEEE Trans. Instrum. Meas. **IM-17**, 395 (1968).
[13] H. Freitag, *Einführung in die Zweitortheorie*, 3rd ed. (Teubner, Stuttgart, 1984), Chap. 12, p. 149.
[14] H. J. Eul and B. Schiek, IEEE Trans. Microwave Theory Tech. **39**, 724 (1991).
[15] A. Enders and G. Nimtz, J. Phys. (France) I **2**, 1693 (1992).
[16] A. Enders and G. Nimtz, J. Phys. (France) I **3**, 1089 (1993).
[17] A. Enders and G. Nimtz, Phys. Rev. B **47**, 9605 (1993).
[18] P. Carpena, V. Gasparian, and M. Ortuño, Phys. Rev. B **51**, 12 813 (1995).
[19] R. Landauer and Th. Martin, Rev. Mod. Phys. **66**, 217 (1994).
[20] E. H. Hauge and J. A. Støvneng, Rev. Mod. Phys. **61**, 917 (1989).
[21] V. S. Olkhovsky and E. Recami, Phys. Rep. **214**, 339 (1992).
[22] A. Enders and G. Nimtz, Phys. Rev. E **48**, 632 (1993).
[23] A. M. Steinberg, P. G. Kwiat, and R. Y. Chiao, Phys. Rev. Lett. **71**, 708 (1993).
[24] G. Nimtz, A. Enders, and H. Spieker, J. Phys. (France) I **4**, 565 (1994).
[25] A. Ranfagni, D. Mugnai, P. Fabeni, and G. P. Pazzi, Appl. Phys. Lett. **58**, 774 (1991).
[26] J. D. Jackson, *Classical Electrodynamics*, 2nd ed. (Wiley, New York, 1975), pp. 301–302.
[27] G. Nimtz, in *Tunneling and its Implications*, Proceedings of the Adratico Research Conference, 1996, edited by D. Mugnai, A. Ranfagni, and L. S. Schulman (World Scientific, Singapore, 1997).
[28] M. Büttiker, Phys. Rev. B **27**, 6178 (1983).
[29] M. Büttiker and R. Landauer, J. Phys. C **21**, 6207 (1988).
[30] V. Gasparian, M. Ortuño, J. Ruiz, and E. Cuevas, Phys. Rev. Lett. **75**, 2312 (1995).
[31] V. Gasparian, M. Ortuño, J. Ruiz, E. Cuevas, and M. Pollak, Phys. Rev. B **51**, 6473 (1995).
[32] W. Jones and N. H. March, *Theoretical Solid State Physics*, 2nd ed. (Dover, New York, 1985), Vol. 1, p. 34.
[33] T. Hattori, N. Tsurumachi, S. Kawato, and Hiroki Nakatsuka, Phys. Rev. B **50**, 4220 (1994).
[34] M. Kohmoto, B. Sutherland, and K. Iguchi, Phys. Rev. Lett. **58**, 2436 (1987).
[35] M. Kohmoto and Y. Oono, Phys. Lett. **102A**, 145 (1984).